



Visualising the urethra for prostate radiotherapy planning

Matthew Richardson, B.Med.Rad.Sc,¹  Kate Skehan, B.Med.Rad.Sc,¹ Lee Wilton, B.Med.Rad.Sc,¹ 
Joshua Sams, B.Med.Rad.Sc,¹ Justin Samuels, B.Med.Rad.Sc,¹ Jonathan Goodwin, PhD,^{1,2}
Peter Greer, PhD,^{1,2} Swetha Sridharan, FRANZCR,¹ & Jarad Martin, FRANZCR^{1,3}

¹Department of Radiation Oncology, Calvary Mater Newcastle, Waratah, New South Wales, Australia

²School of Mathematical and Physical Science, University of Newcastle, Callaghan, New South Wales, Australia

³School of Medicine and Public Health, University of Newcastle, Callaghan, New South Wales, Australia

Keywords

MRI, prostate, radiation therapy, SBRT, urethra

Correspondence

Matthew Richardson, Department of Radiation Oncology, Calvary Mater Newcastle, Waratah, New South Wales 2298, Australia. Tel: +61 240 143 622 (w) | +61 414 584 534 (m); Fax: +61 240 143 128; E-mail: matthew.richardson@calvarymater.org.au

Received: 4 November 2020; Accepted: 1 May 2021

J Med Radiat Sci **68** (2021) 282–288

doi: 10.1002/jmrs.485

Abstract

Introduction: The prostatic urethra is an organ at risk for prostate radiotherapy with genitourinary toxicities a common side effect. Many external beam radiation therapy protocols call for urethral sparing, and with modulated radiotherapy techniques, the radiation dose distribution can be controlled so that maximum doses do not fall within the prostatic urethral volume. Whilst traditional diagnostic MRI sequences provide excellent delineation of the prostate, uncertainty often remains as to the true path of the urethra within the gland. This study aims to assess if a high-resolution isotropic 3D T2 MRI series can reduce inter-observer variability in urethral delineation for radiotherapy planning. **Methods:** Five independent observers contoured the prostatic urethra for ten patients on three data sets; a 2 mm axial CT, a diagnostic 3 mm axial T2 TSE MRI and a 0.9 mm isotropic 3D T2 SPACE MRI. The observers were blinded from each other's contours. A Dice Similarity Coefficient (DSC) score was calculated using the intersection and union of the five observer contours vs an expert reference contour for each data set. **Results:** The mean DSC of the observer vs reference contours was 0.47 for CT, 0.62 for T2 TSE and 0.78 for T2 SPACE ($P < 0.001$). **Conclusions:** The introduction of a 0.9 mm isotropic 3D T2 SPACE MRI for treatment planning provides improved urethral visualisation and can lead to a significant reduction in inter-observer variation in prostatic urethral contouring.

Introduction

Genitourinary (GU) toxicities are a common side effect of prostate radiotherapy.^{1–5} Attempts at correlating bladder dose to GU toxicity have not shown a consistent relationship.⁶ Urethral strictures have long been recognised as a complication of prostate brachytherapy, and as such it is routine practice to try to limit dose delivery to the urethra in modern brachytherapy regimens.^{7,8} Similarly, strictures around the urethral anastomosis are a common concern amongst urologists regarding adjuvant or salvage radiotherapy following a radical prostatectomy.⁹ Although the prostatic urethra has not traditionally been defined as an organ at risk (OAR) for prostate external beam radiation therapy (EBRT), a combination of the above evidence and higher dosed schedules suggests that it would be prudent to

take steps to accurately identify and limit dose to this structure.

Several contemporary ultrahypofractionated prostate EBRT regimes are beginning to call for urethral dose limiting and dose reporting.^{10–12} With modern intensity modulated radiation therapy (IMRT) and volumetric modulated arc therapy (VMAT) techniques combined with online and real-time image-guided radiation therapy (IGRT), the distribution of dose can be controlled so that maximum dose regions do not fall within the prostatic urethral volume whilst still maintaining the minimum therapeutic dose to the entire prostate gland.¹³

Historically, the urethra has been a difficult OAR to accurately define for radiotherapy planning purposes. Ultrasound-based studies have shown the cranio-caudal urethral path and prostatic urethral angle can demonstrate considerable anatomical variations between

subjects.¹⁴ Whilst traditional diagnostic computed tomography (CT) and magnetic resonance imaging (MRI) provide excellent geometrical delineation of the prostate, uncertainty often remains as to the true path of the urethra within the gland itself. Modern ultrahypofractionated trials have permitted an estimated contour of the urethral position with a subsequent radial expansion to create a planning organ at risk volume (PRV).^{10–12} Our institutional planning process historically involved obtaining diagnostic images from external MRI sources and performing a rigid fiducial registration to the planning CT for contouring. A 3 mm axial T2-weighted turbo spin echo (TSE) image provides excellent anatomical contrast and is historically used for target volume and OAR definition.¹⁵ However, the non-isotropic voxels restrict high resolution viewing in the treatment planning system (TPS) to the axial plane only, as shown in Figure 1.

The implementation of ultrahypofractionated stereotactic prostate treatments in our department highlighted the potential benefits of improved urethral visualisation. We initially employed in-dwelling catheters (IDC) at the CT simulation session, followed by a diagnostic T2 TSE MRI with the IDC remaining in situ.¹⁰ This technique provides clear urethral visualisation for dose limiting, but the benefits are confounded by the invasiveness of the procedure, which carries increased infection risk, and is often not well tolerated by patients.^{16,17} This is combined with increased staffing requirements during the simulation sessions. There is also the potential risk with this approach that IDC insertion results in deformation of the natural urethral anatomy,¹⁸ which may be problematic given the IDC was not re-inserted for subsequent treatment appointments.

Studies have shown that a T2-weighted MRI sequence can display the prostatic urethra with hyper-intense contrast compared to the surrounding glandular tissue;

however, the voxel size and slice thickness of the diagnostic series did not provide acceptable multiplane resolution for radiotherapy planning and required specialist urogenital radiologist input.¹⁷ Recent recommendations that a three-dimensional (3D) isotropic T2-weighted axial acquisition is justified for prostate radiation therapy planning have also been published.^{19,20}

We verified that an isotropic T2 SPACE (Sampling Perfection with Application optimised Contrasts using different flip angle Evolution) sequence could produce a 3D prostate image of satisfactory quality for clinical use by our GU radiation oncologists (ROs). We found a 0.9 mm isotropic scan provided optimal image quality for multiplane RT planning (Fig. 2), with a clinically acceptable acquisition time (~5–6 min).

This study investigates the potential impact of implementing an MRI imaging protocol for urethral contouring by assessing inter-observer variability for radiotherapy planning by comparing 3D T2 SPACE, conventional CT and axial T2 TSE MRI planning series.

Methods

Ten male patients with histologically proven prostate carcinoma, an intact prostate gland and who had consented for prostate radiotherapy were identified. All patients provided written informed consent prior to study enrolment. The Hunter New England Human Research Ethics Committee approved this study, reference number 2020/STE01574.

A 120 kV, 2 mm axial CT (SOMATOM CONFIDENCE, Siemens Healthcare, Erlangen, Germany) for treatment planning was acquired in accordance with standard departmental practice and was followed immediately by MRI imaging in the department's dedicated 3-Tesla MRI Simulator (MAGNETOM Skyra, Siemens Healthcare, Erlangen, Germany). For the MRI,

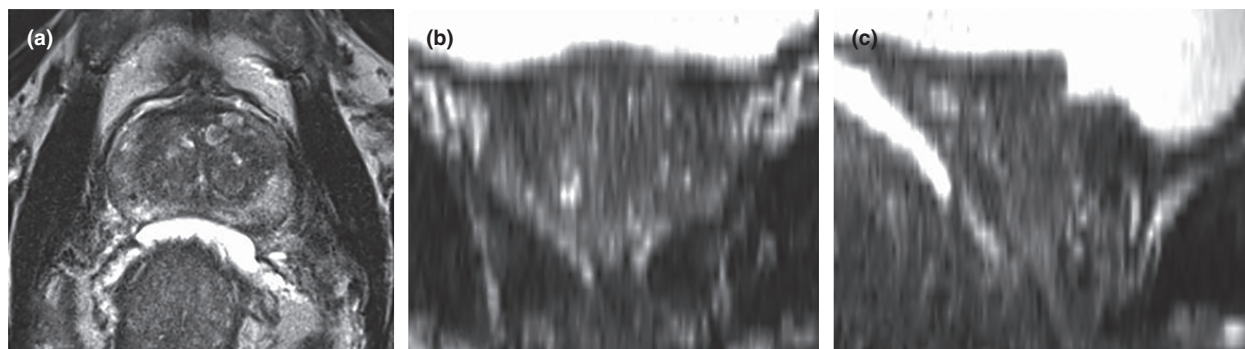


Figure 1. A conventional diagnostic 3 mm T2 TSE series of the prostate as displayed in Eclipse TPS axially (A), and the subsequent degradation in image quality with coronal (B) and sagittal (C) reconstruction.

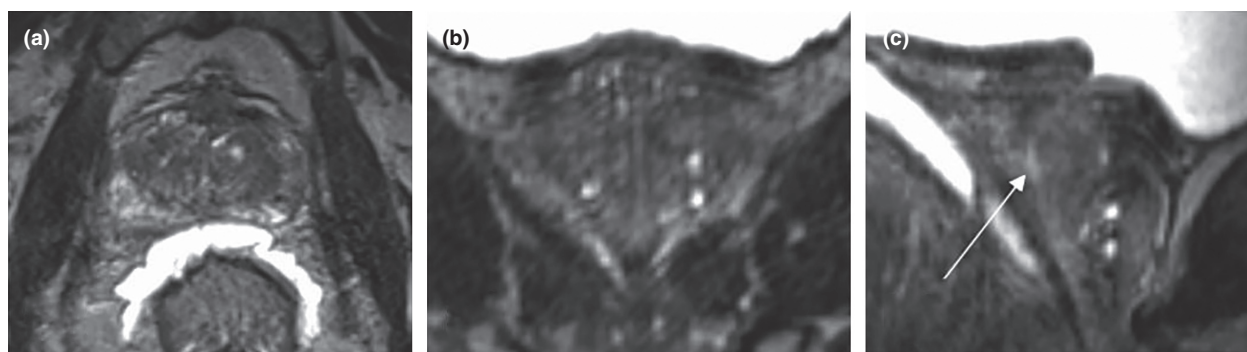


Figure 2. A T2 SPACE series of the prostate as displayed in Eclipse TPS. The 0.9 mm isotropic voxel provides consistent resolution in axial (A) and coronal (B) planes with the arrow indicating the urethra on the sagittal image (C).

patients were immobilised with identical radiotherapy positioning equipment on a QFix Insight™ flat couch overlay with a Siemens Body 18 flex coil fixed to a QFix Insight™ Body Coil Holder. The MR imaging protocol consisted of a 3 mm axial T2 TSE, a 2 mm axial T1 gradient echo (GRE) for fiducial marker visualisation and the additional 0.9 mm isotropic 3D T2 SPACE scan. Table 1 lists the specific MRI acquisition parameters.

All scans were imported into the Eclipse™ treatment planning system (Varian Medical Systems, Palo Alto, CA, USA), and rigid registration of CT, T1 GRE, T2 TSE and T2 SPACE using gold seed fiducial markers was performed for each patient. The clinical target volume (CTV) was contoured by the RO on the CT using the T2 TSE series in a blended window as per current clinical practice. The CTV was duplicated onto each T2-weighted series. The radiation oncologist created a reference urethral PRV contour in consensus with a GU clinical specialist radiation therapist using both T2-weighted series via the prescribed method below. The reference contour was copied to all three data sets and approved as a clinically acceptable urethral position.

Table 1. MRI acquisition parameters.

Parameter	T2	T2	T1
Sequence type	2D Axial TSE	3D SPACE TSE	GRE
TE (ms)	104	102	6.66
TR (ms)	8030	1700	689
Flip angle (°)	196	150	80
FOV (mm)	160	220	220
Slice thickness (mm)	3	0.9	2
Resolution matrix	384 × 384	233 × 256	256 × 320

GRE = gradient echo; TSE = turbo spin echo; SPACE = sampling perfection with application optimised contrast using different flip angle evolution; TE = echo time; TR = repetition time; FOV = field of view.

Five radiation therapists (with a range of 5–19 years experience) sub-specialising in GU radiation therapy contoured the prostatic urethra of the ten patients on each data set; planning CT, T2 TSE and the T2 SPACE series using the same prescribed method. The observers were blinded to all other urethra contours. The data sets were contoured in the above sequential order.

On each series, the observers were instructed to contour the urethra within the CTV volume in the sagittal window from bladder neck to the apex of the prostate using the 3D brush tool set to a static 2 mm diameter (Fig. 3). The urethra contour was drawn on the sagittal plane, with the axial and coronal planes also available for viewing to help guide the observer in all series. The urethra contours were set as ‘high resolution structures’ in the contour properties. Contouring of the urethra across multiple sagittal slices was permitted if the urethral path appeared convoluted through the prostate gland. Any large transurethral resection of the prostate (TURP) voids were also contoured as part of the prostatic urethra if they fell inside the CTV volume. In order to create a conventional cylindrical urethral PRV, a further 3 mm radial expansion was applied to the contours. Any volume extending outside of the CTV in the superior–inferior direction was cropped. The final ~8-mm-diameter cylindrical urethra PRV structure was then used for analysis.

A further two contours were then created for every observer on each of the three imaging methods for the ten patients. This consisted of (a) the intersecting volume of the observer and reference contour ($A \cap B$) and (b) the union of the observer contour and the reference contour ($A \cup B$). The diagram in Figure 4 represents the volumes created for each observer contour vs the reference contour.

The volume of the intersection and union contours was recorded. A Dice Similarity Coefficient (DSC) was

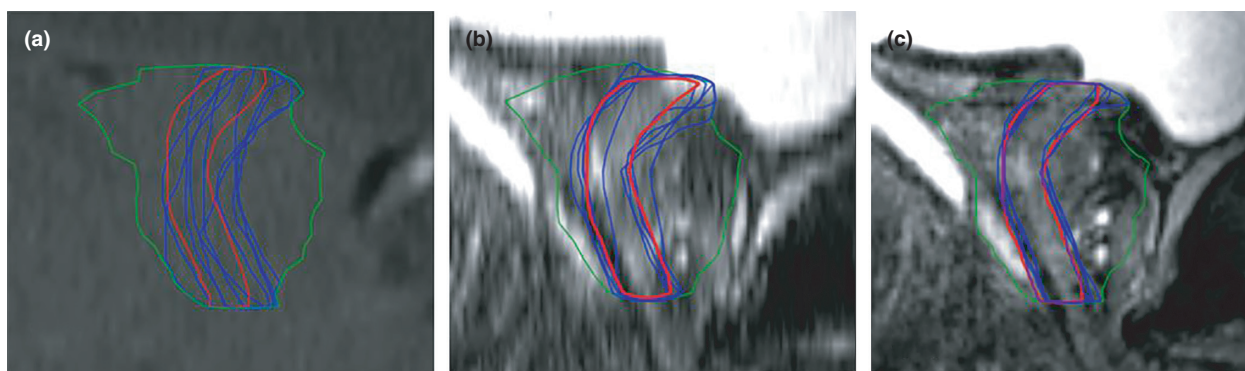


Figure 3. Sagittal example of one patient data set with observer urethra PRV contours (blue) and reference contour (red) for CT (A), T2 TSE (B) and T2 SPACE (C).

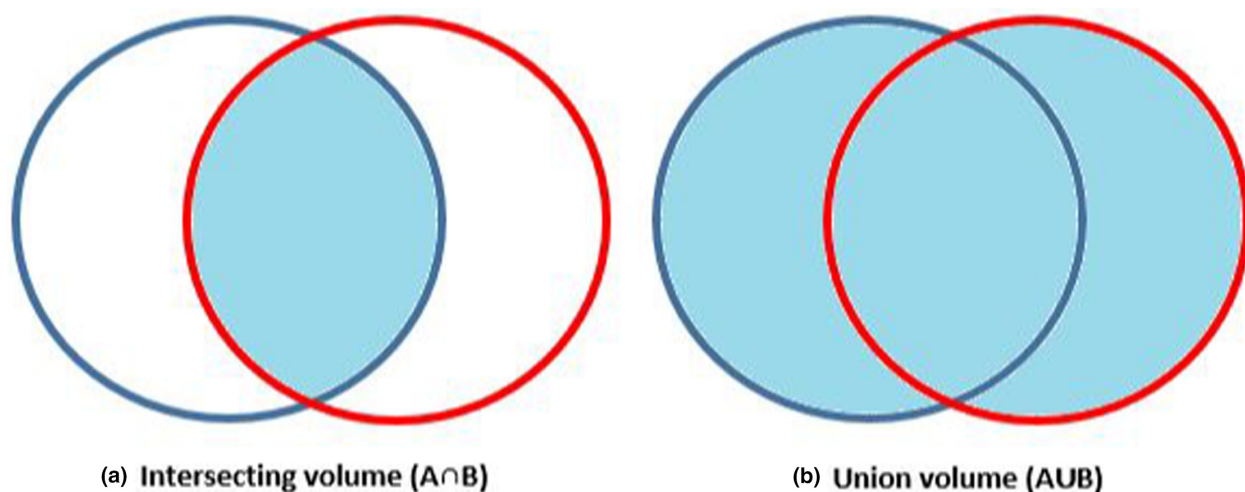


Figure 4. Shaded regions representing volumes created for DSC scoring; (a) intersecting volume of observer & reference contour ($A \cap B$) & (b) union of observer and reference contour ($A \cup B$).

calculated using the equation; $DSC = 2 (A \cap B) / (A \cup B)$. The DSC score was then used to assess the inter-observer similarity of the identified urethral volumes. DSC comparisons have been widely used as a metric to evaluate spatial overlap between multiple volumes in radiation oncology settings.^{21–24} DSC scores are displayed as a value between 0 – representing no spatial overlap, and 1 – representing perfect spatial overlap. A DSC score of >0.70 has been reported as demonstrating ‘good’ spatial and volumetric similarity.²⁵

Two factor statistical analysis was performed using Friedman’s two-way repeated ANOVA to assess main effect difference, based on ten patients and three image acquisition types for five independent observers. Subsequent post hoc multiple comparison was performed using Fisher’s Least Significant Difference test to compare each pair of the three different imaging methods.

Results

The mean DSC of the observer vs reference contours was 0.47 for CT, 0.62 for T2 TSE and 0.78 for T2 SPACE, as shown in Table 2. The calculated Friedman’s two-way repeated ANOVA P -value of <0.001 suggests that there is a significant overall difference between the three groups. DSC scores improved from CT to T2 TSE (mean DSC improvement = +0.15), and then further improvements were seen in the T2 TSE to T2 SPACE comparison (mean DSC improvement = +0.16).

Post hoc multiple comparison of the three groups resulted in: CT-T2 TSE $P = 0.23$; CT-T2 SPACE $P = <0.001$; T2 TSE-T2 SPACE $p = 0.023$. These results demonstrate a significant difference in mean value between T2 SPACE when compared to both T2 TSE and CT DSC groups.

Table 2. Mean Dice Similarity Coefficient (DSC) of observer contours ($n = 5$) vs reference contour.

Patient no.	CT	T2 TSE	T2 SPACE
1	0.384	0.752	0.863
2	0.68	0.788	0.893
3	0.352	0.452	0.773
4	0.533	0.55	0.675
5	0.539	0.65	0.724
6	0.474	0.673	0.806
7	0.401	0.727	0.812
8	0.508	0.574	0.772
9	0.423	0.446	0.769
10	0.446	0.625	0.738
Mean	0.474	0.624	0.783
Minimum	0.352	0.446	0.675
Maximum	0.680	0.788	0.893

A graphical representation in Figure 5 shows clear improvements in DSC score for T2 SPACE compared to the conventional imaging series.

Discussion

This study has demonstrated that the improvement in image quality achieved through the use of a 0.9 mm isotropic 3D T2 SPACE sequence can result in less inter-observer variability in contouring of the prostatic urethra PRV, when compared to conventional CT and diagnostic

T2 TSE MRI approaches. Note that no patient had a better mean DSC for the T2 TSE compared to the T2 SPACE approach. The authors acknowledge this study involves a relatively small patient cohort and the results presented pertain to the observers in this study and may not generalise to other observers. However, the consistency and strong statistical evidence of the results suggest it is unlikely that more patients would lead to a change in outcome, particularly in relation to T2 SPACE vs convention planning CT, where a highly significant difference was observed between mean DSC ($P < 0.001$).

Whilst the T2 SPACE series does show reduced inter-observer variability, contouring the urethra can still require a degree of estimation. Patients with a convoluted urethral path or large body habitus may still be difficult to visualise. Conversely, patients with significant TURP voids could likely be contoured accurately with a standard T2 TSE diagnostic series alone, and this was observed in patient #5 in the cohort. During the course of this investigation, the significance of ensuring a quality patient set-up has been reinforced with an anatomically straight and level pelvis showing obvious improvement in urethral visualisation. Also of note, the increased scan acquisition time of T2 SPACE compared to T2 TSE (2–3 min) can introduce motion artefact, with patient discomfort from bladder filling a potential factor. Furthermore, contouring on an MR image in the sagittal viewing plane of the TPS may be a novel technique for some as the axial plane has long been the primary

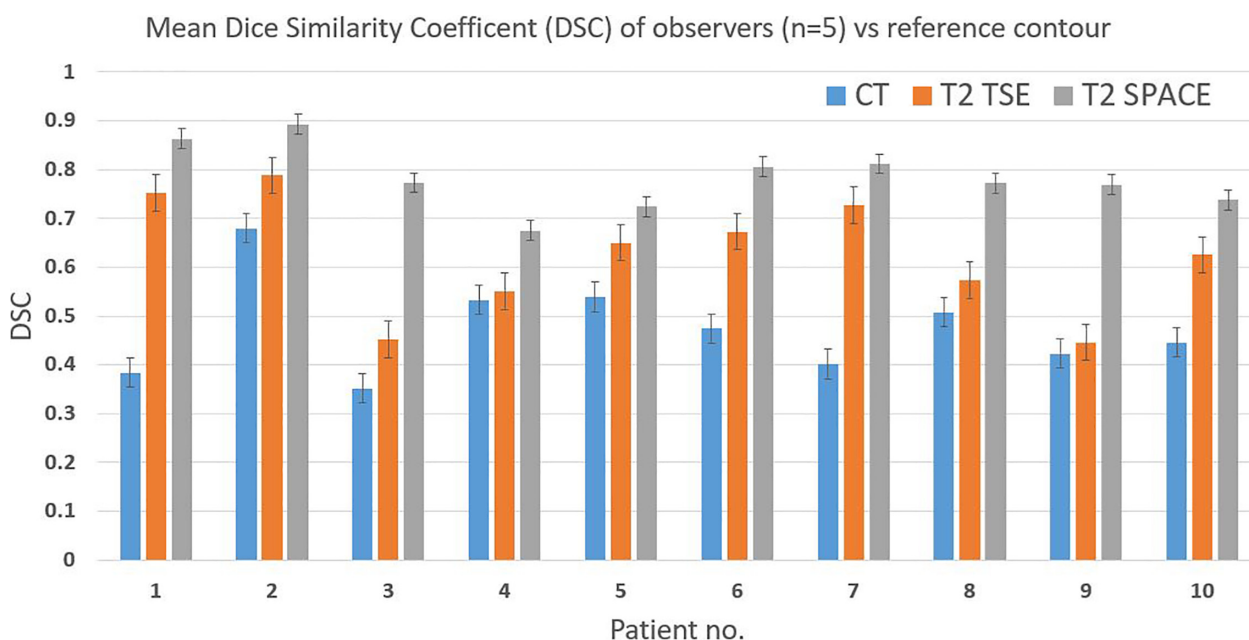


Figure 5. Graphical representation of mean DSC scores showing a reduction in inter-observer variation for T2 SPACE.

viewing window for RT contouring and planning. Therefore, protocol-based user education is critical to ensure best value is obtained from its implementation.²³

The alternative approach of placing an IDC is also sometimes deployed for ultrahypofractionated regimens, with some protocols exploring cooling of the urethra.¹³ That said, the rate of moderate-to-severe GU toxicity appears to be low with RT doses <40 Gy in 5 fractions delivered without any specific urethral sparing.^{26,27} As such, the main advantages of such an approach are likely to be in emerging indications such as boosting of the dominant intraprostatic nodule (DIL), prostate re-irradiation and further dose escalation such as on virtual HDR boost protocols.^{28–31} Patients with intraprostatic recurrence after radiotherapy can be managed with re-irradiation³² and may benefit from a more reliable approach to urethral delineation as meticulous attention to urethral doses is often mandated in the SBRT retreatment scenario.³³ By reducing the inherent uncertainty around the urethral PRV and using a consistent contouring approach, we see potential to more confidently investigate future urethral dose sparing opportunities.

Recommendations to tailor MRI imaging protocols towards a radiotherapy focus have been reported and have the potential to provide tangible benefit to patients undergoing radiotherapy.²⁰ The installation of a dedicated MRI simulator continues to expedite these adaptations for our department. It opens the scope to an MRI only planning process, which is a current research focus in our unit.³⁴ The authors also feel that this small study supports the need for multidisciplinary collaboration to best utilise the MRI for quality improvement in day-to-day radiotherapy imaging.³⁵

Conclusion

The introduction of a 0.9 mm isotropic 3D T2 SPACE planning MRI provides improved urethral visualisation and can lead to a marked reduction in inter-observer variation of prostatic urethral contours compared to conventional planning CT and diagnostic T2 TSE MRI. The improvements in urethral visualisation were best appreciated in the sagittal plane in the TPS. We have adopted the T2 SPACE as a standard contouring sequence for prostate radiotherapy planning in the MRI simulator.

Acknowledgments

The authors do not have any financial grants, industrial links or affiliations to declare.

Conflict of Interest

The authors declare no conflict of interest.

References

- Denham JW, Steigler A, Joseph D, et al. Radiation dose escalation or longer androgen suppression for locally advanced prostate cancer? Data from the TROG 03.04 RADAR trial. *Radiother Oncol* 2015; **115**: 301–7.
- Elliott SP, Malaeb BS. Long-term urinary adverse effects of pelvic radiotherapy. *World J Urol* 2011; **29**: 35–41.
- Dearnaley D, Syndikus I, Mossop H, et al. Conventional versus hypofractionated high-dose intensity-modulated radiotherapy for prostate cancer: 5-year outcomes of the randomised, non-inferiority, phase 3 CHHiP trial. *Lancet Oncol* 2016; **17**: 1047–60.
- Widmark A, Gunnlaugsson A, Beckman L, et al. Ultra-hypofractionated versus conventionally fractionated radiotherapy for prostate cancer: 5-year outcomes of the HYPO-RT-PC randomised, non-inferiority, phase 3 trial. *The Lancet* 2019; **394**: 385–95.
- Zelevsky MJ, Kollmeier M, McBride S, et al. Five-year outcomes of a phase 1 dose-escalation study using stereotactic body radiosurgery for patients with low-risk and intermediate-risk prostate cancer. *Int J Radiat Oncol Biol Phys* 2019; **104**: 42–9.
- Viswanathan AN, Yorke ED, Marks LB, Eifel PJ, Shipley WU. Radiation dose volume effects of the urinary bladder. *Int J Radiat Oncol Biol Phys* 2010; **76**: S116–122.
- Morris WJ, Tyldesley S, Rodda S, et al. Androgen suppression combined with elective nodal and dose escalated radiation therapy (the ASCENDE-RT Trial): an analysis of survival endpoints for a randomized trial comparing a low-dose-rate brachytherapy boost to a dose-escalated external beam boost for high- and intermediate-risk prostate cancer. *Int J Radiat Oncol Biol Phys* 2017; **98**: 275–85.
- Sullivan L, Williams SG, Tai KH, Foroudi F, Cleeve L, Duchesne GM. Urethral stricture following high dose rate brachytherapy for prostate cancer. *Radiother Oncol* 2009; **91**: 232–6.
- Gandaglia G, Briganti A, Clarke N, et al. Adjuvant and salvage radiotherapy after radical prostatectomy in prostate cancer patients. *Eur Urol* 2017; **72**: 689–709.
- Richardson M, Sidhom M, Gallagher S, et al. PROstate Multicentre External beam radioTHERapy Using a Stereotactic boost: the PROMETHEUS study protocol. *BMC Cancer* 2018; **18**: 588.
- Keall P, Nguyen DT, O'Brien R, et al. Stereotactic prostate adaptive radiotherapy utilising kilovoltage intrafraction monitoring: the TROG 15.01 SPARK trial. *BMC Cancer* 2017; **17**: 180.
- Martin J, Keall P, Siva S, et al. TROG 18.01 phase III randomised clinical trial of the Novel Integration of New

- prostate radiation schedules with adjuvant Androgen deprivation: NINJA study protocol. *BMJ Open* 2019; **9**: e030731.
13. Jaccard M, Zilli T, Dubouloz A, et al. Urethra-sparing stereotactic body radiation therapy for prostate cancer: quality assurance of a randomized phase 2 trial. *Int J Radiat Oncol Biol Phys* 2020; **108**: 1047–54.
 14. Hou CP, Chen C-L, Lin Y-H, et al. Prostatic urethral angle might be a predictor of treatment efficacy of alpha-blockers in men with lower urinary tract symptoms. *Drug Des Devel Ther* 2014; **8**: 937–43.
 15. Barentsz JO, Richenberg J, Clements R, et al. ESUR prostate MR guidelines 2012. *Eur Radiol* 2012; **22**: 746–57.
 16. Saint S, Lipsky BA, Goold SD. Indwelling urinary catheters: a one-point restraint? *Ann Intern Med* 2002; **137**: 125–7.
 17. Kataria T, Gupta D, Goyal S, et al. Simple diagrammatic method to delineate male urethra in prostate cancer radiotherapy: an MRI based approach. *Br J Radiol* 2016; **89**: 20160348.
 18. Maenhout M, van der Voort van Zyp JRN, Borot de Battisti M, et al. The effect of catheter displacement and anatomical variations on the dose distribution in MRI-guided focal HDR brachytherapy for prostate cancer. *Brachytherapy* 2018; **17**: 68–77.
 19. Menard C, Paulson E, Nyholm T, et al. Role of prostate MR imaging in radiation oncology. *Radiol Clin North Am* 2018; **56**: 319–25.
 20. Speight R, Schmidt MA, Liney GP, et al. IPEM topical report: guidance on the use of MRI for external beam radiotherapy treatment planning. *Phys Med Biol* 2021; **64**: 175021.
 21. Dowling JA, Sun J, Pichler P, et al. Automatic substitute computed tomography generation and contouring for magnetic resonance imaging (MRI)-alone external beam radiation therapy from standard MRI sequences. *Int J Radiat Oncol Biol Phys* 2015; **93**: 1144–53.
 22. Wang K, Mullins BT, Falchook AD, et al. Evaluation of PET/MRI for tumor volume delineation for head and neck cancer. *Front Oncol* 2017; **7**: 8.
 23. Khoo EL, Schick K, Plank AW, et al. Prostate contouring variation: can it be fixed? *Int J Radiat Oncol Biol Phys* 2012; **82**: 1923–9.
 24. Vinod SK, Jameson MG, Min M, Holloway LC. Uncertainties in volume delineation in radiation oncology: a systematic review and recommendations for future studies. *Radiother Oncol* 2016; **121**: 169–79.
 25. Zou K, Warfield S, Bharatha A, et al. Statistical validation of image segmentation quality based on a spatial overlap index. *Acad Radiol* 2004; **11**: 178–89.
 26. Keall P, Nguyen DT, O'Brien R, et al. Real-time image guided ablative prostate cancer radiation therapy: results from the TROG 15.01 SPARK trial. *Int J Radiat Oncol Biol Phys* 2020; **107**: 530–8.
 27. Kishan AU, Dang A, Katz AJ, et al. Long-term outcomes of stereotactic body radiotherapy for low-risk and intermediate-risk prostate cancer. *JAMA Netw Open* 2019; **2**: e188006.
 28. Draulans C, van der Heide UA, Haustermans K, et al. Primary endpoint analysis of the multicentre phase II hypo-FLAME trial for intermediate and high risk prostate cancer. *Radiother Oncol* 2020; **147**: 92–8.
 29. Bergamin S, Eade T, Kneebone A, et al. Interim results of a prospective prostate-specific membrane antigen-directed focal stereotactic reirradiation trial for locally recurrent prostate cancer. *Int J Radiat Oncol Biol Phys* 2020; **108**: 1172–8.
 30. Pryor D, Sidhom M, Arumugam S, et al. Phase 2 multicenter study of gantry-based stereotactic radiotherapy boost for intermediate and high risk prostate cancer (PROMETHEUS). *Front Oncol* 2019; **9**: 217.
 31. Kerkmeijer LGW, Groen VH, Pos FJ, et al. Focal boost to the intraprostatic tumor in external beam radiotherapy for patients with localized prostate cancer: results from the FLAME randomized phase III trial. *J Clin Oncol* 2021; **39**: 787–96.
 32. Baty M, Créhange G, Pasquier D, et al. Salvage reirradiation for local prostate cancer recurrence after radiation therapy. For who? When? How? *Cancer Radiother* 2019; **23**: 541–58.
 33. David Pasquier M-CLD, Tresch E, Cormier L, Martine Duterque SN, Lartigau E. GETUG-AFU 31: a phase I/II multicentre study evaluating the safety and efficacy of salvage stereotactic radiation in patients with intraprostatic tumour recurrence after external radiation therapy—study protocol. *BMJ Open* 2019; **9**: e026666.
 34. Greer P, Martin J, Sidhom M, et al. A multi-center prospective study for implementation of an MRI-only prostate treatment planning workflow. *Front Oncol* 2019; **9**: 826.
 35. Rai R, Kumar S, Batumalai V, et al. The integration of MRI in radiation therapy: collaboration of radiographers and radiation therapists. *J Med Radiat Sci* 2017; **64**: 61–8.